

A next-to-next-to-leading-order $pp \rightarrow pp\pi^0$ Transition Operator in Chiral Perturbation Theory

V. Dmitrašinović^a, K. Kubodera^a, F. Myhrer^a and T. Sato,^b

^a *Department of Physics and Astronomy, University of South Carolina
Columbia, SC 29208, U. S. A.*

^b *Department of Physics, Osaka University, Toyonaka, Osaka 560-0043, Japan*
(February 9, 2020)

Abstract

We present a systematic analysis of next-to-next-to-leading-order diagrams that contribute to the $pp \rightarrow pp\pi^0$ production at threshold. Analytic expressions are given for the effective transition operators, and the relative importance of various types of diagrams is discussed. The vertex-correction-type graphs are found to give only small corrections to lower order graphs in conformity with expectations. By contrast, we find very large contributions from two-pion exchange graphs that can be interpreted as a part of effective σ -meson exchange diagrams. The recoil correction to the pion rescattering diagram also turns out to be large.

PACS numbers: 25.40.Ep, 25.40.Qa, 12.39.Fe

a. Introduction High-precision measurements [1,2] of neutral pion production in proton-proton collisions $pp \rightarrow pp\pi^0$ just above the threshold have generated renewed theoretical scrutiny of this reaction [3]- [16]. This reaction is unique among two-nucleon pion production processes in that it is not well described by the single-nucleon process (Born term), Fig.1(a), and the s-wave pion rescattering process, Fig.1(b). The reason is that the “large” Weinberg-Tomozawa term does not contribute to the $pp \rightarrow pp\pi^0$ reaction, in contrast with e.g. charged-pion production $pp \rightarrow pn\pi^+$, thus rendering $pp \rightarrow pp\pi^0$ particularly sensitive to and hence an interesting testing ground for the less-well-understood “small” isoscalar s-wave pion rescattering terms. From the calculations done thus far it is clear that the two most basic processes, Fig.1(a) and 1(b), give much smaller $pp \rightarrow pp\pi^0$ cross sections than the measured values. Lee and Riska’s model calculation [4] suggests that shorter-range isoscalar meson-exchange processes, like σ - and ω - exchanges between the two protons, might be very important in this reaction.

In heavy-baryon chiral perturbation theory [HB χ PT] [17] one can define the “large” and “small” terms in the Hamiltonian by way of chiral-order counting. In this language the first pion rescattering contributions to $pp \rightarrow pp\pi^0$ are one chiral-order higher than those of the charged-pion production (e.g., $pp \rightarrow pn\pi^+$). This means that $pp \rightarrow pp\pi^0$ production is very sensitive to “correction terms”, which tend to be “masked” by the leading terms in most low-energy pion-nucleon processes. Since the Born term and the pion rescattering term do not explain the $pp \rightarrow pp\pi^0$ cross section, we extend here our previous calculation [13] to the next chiral order.

It must be mentioned, however, that application of HB χ PT to the $NN \rightarrow NN\pi$ processes is a delicate matter in at least two aspects. First, the non-negligible energy-momentum transfers involved can make less clear the distinction between reducible and irreducible diagrams in Weinberg’s chiral counting scheme. This has led Cohen *et al.* [14] to propose new counting rules to be used for inelastic processes like $NN \rightarrow NN\pi$. It is noteworthy that in this modified scheme loop diagrams can be of the lowest order. Secondly, as the nucleon recoil involved becomes appreciable, the static nucleon “propagator”, which is one of the basic features of the HB χ PT formalism, can become increasingly problematic. Meanwhile, “improving” the HB χ PT propagator by including a nucleon recoil term requires an extension of HB χ PT from its original form. Despite the importance of these issues, we postpone the discussion of these matters to a future publication. In this Letter we rather use the standard counting rules à la Weinberg [18] within the framework of HB χ PT. We concentrate on calculations of the effective transition operators strictly within the narrow definition of HB χ PT. We also relegate to the future the consideration of the initial- and final-state interactions in the transition amplitude, even though we are aware of the paramount importance of a full distorted-wave (DW) calculation for comparison with the experiment. This is, for one thing, because the transition operators resulting from our systematic treatment of the new diagrams exhibit very complicated energy- and momentum-dependencies, rendering a full DW calculation a highly non-trivial numerical task. Secondly, we wish to separate out the effects of higher-order diagrams in the “kernel” (irreducible part) of the reaction from the perhaps more mundane yet numerically important initial- and final-state interaction effects.

The principal purpose of this note is to report analytic results for the transition operators that arise from a systematic treatment of the next chiral order diagrams in HB χ PT. In order to gain some insight into the relative numerical significance of these diagrams, we compare

their absolute values, at the threshold, to that of the one-pion exchange rescattering graph, Fig.1(b). Our most important finding is that some of the two-pion exchange diagrams, which have no lower-order counterparts, give by far the dominant transition operators at the threshold (sometimes by an order of magnitude larger than the nominally “leading” ones). These new diagrams may be interpreted as a part of an effective σ -meson exchange (see below).

b. Conventions and other preliminaries The effective Lagrangian \mathcal{L}_{ch} in HB χ PT is expanded as

$$\mathcal{L}_{\text{ch}} = \mathcal{L}^{(0)} + \mathcal{L}^{(1)} + \mathcal{L}^{(2)} + \dots \quad (1)$$

$\mathcal{L}^{(\bar{\nu})}$ represents a term of chiral order $\bar{\nu}$ with $\bar{\nu} \equiv d + (n/2) - 2$, where n is the number of fermion fields in the term, and d is the number of derivatives or powers of m_π . The explicit forms for the $\bar{\nu} = 0$ and 1 terms are [20]:

$$\mathcal{L}^{(0)} = \frac{f_\pi^2}{4} \text{Tr}[\partial_\mu U^\dagger \partial^\mu U + m_\pi^2(U^\dagger + U - 2)] + \bar{N}(iv \cdot D + g_A S \cdot u)N \quad (2)$$

$$\begin{aligned} \mathcal{L}^{(1)} = & -\frac{ig_A}{2m_N} \bar{N}\{S \cdot D, v \cdot u\}N + 2c_1 m_\pi^2 \bar{N}N \text{Tr}(U + U^\dagger - 2) \\ & + (c_2 - \frac{g_A^2}{8m_N}) \bar{N}(v \cdot u)^2 N + c_3 \bar{N}u \cdot u N + \dots \end{aligned} \quad (3)$$

where we have retained only terms of direct relevance to our present calculation. The SU(2) field matrix $U(x)$ is non-linearly related to the pion field and has standard chiral transformation properties. We use the representation $U(x) = \sqrt{1 - [\boldsymbol{\pi}(x)/f_\pi]^2} + i\boldsymbol{\tau} \cdot \boldsymbol{\pi}(x)/f_\pi$ as in Ref. [20]. $N(x)$ represents the large component of the heavy-nucleon field; the four-velocity parameter v_μ is chosen to be $v_\mu = (1, 0, 0, 0)$; $D_\mu N = (\partial_\mu + \frac{1}{2}[\xi^\dagger, \partial_\mu \xi])N$ is the covariant derivative of N ; S_μ is the (covariant) spin operator, which in the nucleon rest frame becomes $S^\mu = (0, \vec{\sigma}/2)$, and $u_\mu = i[\xi^\dagger \partial_\mu \xi - \xi \partial_\mu \xi^\dagger]$, where $\xi = \sqrt{U(x)}$ [20]. The low-energy constants c_1, c_2 and c_3 have been determined from other processes, see e.g. Refs. [15,20]. An explicit expression for $\mathcal{L}^{(2)}$, which includes $\mathcal{O}(m_N^{-2})$ recoil terms as well as terms containing new low-energy constants, can be found, e.g., in Ref. [21].

In Weinberg’s chiral counting [18] each irreducible Feynman diagram carries a chiral order index ν defined by $\nu = 4 - E_N - 2C + 2L + \sum_i \bar{\nu}_i$, where E_N is the number of nucleons in the Feynman diagram, L the number of loops, C the number of disconnected parts of the diagram, and the sum runs over all the vertices in the Feynman graph [18]. In this note we consider irreducible diagrams with chiral orders up to $\nu = 2$ that give rise to $pp \rightarrow pp\pi^0$ transition operators. These diagrams are shown in Figs. 1-5. In the following $\mathcal{T}^{(\nu)}$ stands for a transition operator of chiral order ν . The lowest-order transition operator for the Born diagram [Fig.(1a)] has $\nu = -1$, and that for the rescattering diagram has $\nu = +1$ [Fig.(1b)]. We define the first HB χ PT calculation [13,14] which includes the aforementioned terms as the next-to-leading (NLO) calculation. Hence we decree our next chiral order ($\nu = 2$) calculation to be next-to-next-to-leading (NNLO) order. With the use of \mathcal{L}_{ch} in Eq.(1), the two transition operators that feature in the NLO calculation are given (in momentum space) by [13,14]

$$\mathcal{T}^{Born} = \mathcal{T}^{(\nu=-1)} = \frac{g_A}{2f_\pi} \sum_{j=1,2} \frac{\omega_q}{2m_N} \vec{\sigma}_j \cdot (\vec{p}_j + \vec{p}_j') \tau_j^0, \quad (4)$$

$$\mathcal{T}^{Resc} = \mathcal{T}^{(\nu=+1)} = \left(\frac{-g_A}{f_\pi} \right) \sum_{j=1,2} \kappa(k_j, q) \frac{\vec{\sigma}_j \cdot \vec{k}_j \tau_j^0}{k_j^2 - m_\pi^2 + i\eta}, \quad (5)$$

where \vec{p}_j and \vec{p}_j' ($j = 1, 2$) denote the initial and final momenta of the j -th proton. The four-momentum of the exchanged pion is defined by the nucleon four-momenta at the πNN vertex: $k_j \equiv p_j - p_j'$, where $p_j = (E_{p_j}, \vec{p}_j)$, $p_j' = (E_{p_j'}, \vec{p}_j')$ with the definition $E_p = (\vec{p}^2 + m_N^2)^{1/2} - m_N$. The s-wave rescattering vertex function $\kappa(k, q)$ is calculated from Eq.(3):

$$\kappa(k, q) \equiv \frac{m_\pi^2}{f_\pi^2} \left(2c_1 - (c_2 - \frac{g_A^2}{8m_N}) \frac{\omega_q k_0}{m_\pi^2} - c_3 \frac{q \cdot k}{m_\pi^2} \right), \quad (6)$$

where $k = (k_0, \vec{k})$ and $q = (\omega_q, \vec{q})$ represent the four-momenta of the exchanged and final pions, respectively, and $\omega_q = (\vec{q}^2 + m_\pi^2)^{1/2}$.

c. Analytic results When we consider NNLO, we find 19 topologically distinct new types of diagrams that can potentially contribute to $NN \rightarrow NN\pi$ reactions. For a particular case of the $pp \rightarrow pp\pi^0$ reaction near threshold, the isospin selection rules and the s-wave character of the outgoing pion reduce this number from 19 to 6. We refer to these six as Type I, Type II, ..., Type VI, and illustrate them in Figs. 2-4. Types I, II and III appear in Fig. 2, Type IV in Fig. 3, and Types V and VI in Fig.4. Some of these diagrams have been considered by Gedalin *et al.* [22], as we shall discuss later. We denote by M_I, M_{II}, \dots , the NNLO transition operators that arise from the diagrams of Type I, II,..., respectively. In addition to these six operators, as will be explained in more detail below, there is an NNLO contribution from Fig. 5, which looks the same as Fig. 1(b), but which constitutes a higher-order correction to $\mathcal{T}^{(+1)}$ [eq.(5)]. We denote by M_{VII} the transition operator due to this correction. Then the total NNLO transition operator we consider is given by

$$\mathcal{T}^{(+2)} = M_I + M_{II} + M_{III} + M_{IV} + M_V + M_{VI} + M_{VII}. \quad (7)$$

The explicit expressions for these operators are as follows. (In the expressions below the subscripts i and j refer to nucleon number 1 and 2.)

$$M_I = \frac{g_A}{8f_\pi^5} \sum_{i \neq j=1,2} S_i \cdot k_j [X_1 + \frac{X_2}{k_j^2}] \quad (8)$$

where

$$\begin{aligned} X_1 &= v \cdot (p_i + p_i') I_\pi(k_j) + v \cdot (q + \frac{p_i'}{2}) v \cdot (q + p_i + p_i') I_0(v \cdot p_i, -v \cdot k_j, k_j^2) + \\ &\quad + v \cdot (q - \frac{p_i}{2}) v \cdot (q - p_i - p_i') I_0(v \cdot p_i', v \cdot k_j, k_j^2) \\ X_2 &= -v \cdot (p_i + p_i') v \cdot (5q - k_i) v \cdot k_j I_\pi(k_j) - v \cdot (q + \frac{p_i'}{2}) v \cdot (q + p_i + p_i') \times \\ &\quad \times [J_0(v \cdot p_i) - J_0(v \cdot (p_i + k_j)) + v \cdot k_j v \cdot (k_j + 2p_i) I_0(v \cdot p_i, -v \cdot k_j, k_j^2)] + \\ &\quad - v \cdot (q - \frac{p_i}{2}) v \cdot (q - p_i - p_i') [J_0(v \cdot p_i') - J_0(v \cdot (p_i' - k_j)) + v \cdot k_j v \cdot (k_j - 2p_i') I_0(v \cdot p_i', v \cdot k_j, k_j^2)]. \end{aligned} \quad (9)$$

$$M_{\text{II}} = \frac{g_A^3}{8f_\pi^5} \sum_{i \neq j=1,2} S_i \cdot (k_j - k_i) \{ J_0(v \cdot p_j) + J_0(v \cdot p'_j) + v \cdot (p_j + p'_j) I_\pi(k_j) + \\ + (-2m_\pi^2 + 2v \cdot p_j v \cdot p'_j + k_j^2) I_0(v \cdot p'_j, -v \cdot k_j, k_j^2) \}. \quad (11)$$

$$M_{\text{III}} = \frac{g_A^3}{4f_\pi^5} \sum_{i \neq j=1,2} [S_i \cdot k_j \bar{X}_1 + 2i\epsilon_{\mu\nu\alpha\beta} v^\alpha S_j^\beta S_i^\mu k_j^\nu \bar{X}_2], \quad (12)$$

where

$$\bar{X}_1 = -v \cdot (p_i + p_j + p'_i + p'_j) \frac{1}{2} I_\pi(k_j) + \\ + \frac{1}{v \cdot (p_i - p'_j)} [v \cdot (p_i + q + k_j) \mathcal{Y}(v \cdot p_i, -k_j) - v \cdot (p'_j + q + k_j) \mathcal{Y}(v \cdot p'_j, -k_j)] + \\ + \frac{1}{v \cdot (p'_i - p_j)} [v \cdot (p'_i - q - k_j) \mathcal{Y}(v \cdot p'_i, k_j) - v \cdot (p_j - q - k_j) \mathcal{Y}(v \cdot p_j, k_j)] \quad (13)$$

$$\bar{X}_2 = \frac{1}{v \cdot (p_i - p'_j)} [v \cdot (p_i + q + k_j) \mathcal{A}(v \cdot p_i, -k_j) - v \cdot (p'_j + q + k_j) \mathcal{A}(v \cdot p'_j, -k_j)] + \\ - \frac{1}{v \cdot (p'_i - p_j)} [v \cdot (p'_i - q - k_j) \mathcal{A}(v \cdot p'_i, k_j) - v \cdot (p_j - q - k_j) \mathcal{A}(v \cdot p_j, k_j)]. \quad (14)$$

In Eqs.(13) and (14):

$$\mathcal{Y}(\omega, P) = \\ \frac{1}{4} [4(v \cdot P) I_\pi(P) - J_0(\omega) - J_0(\omega - v \cdot P) + (2m_\pi^2 - 2(\omega - v \cdot P)^2 + \vec{P}^2) I_0(\omega, v \cdot P, P^2)] + \\ + \left(\frac{[2m_\pi^2 - \omega^2 - (\omega - v \cdot P)^2]}{4\vec{P}^2} \right) \times \\ \times [2(v \cdot P) I_\pi(P) - J_0(\omega) + J_0(\omega - v \cdot P) + (v \cdot P)(2\omega - v \cdot P) I_0(\omega, v \cdot P, P^2)], \quad (15)$$

and

$$\mathcal{A}(\omega, P) = \frac{(2\omega - v \cdot P)P^2}{4\vec{P}^2} I_\pi(P) + \\ + \left(\frac{m_\pi^2}{2} + \frac{P^2[P^2 + 4\omega^2 - 4\omega(v \cdot P)]}{8\vec{P}^2} \right) I_0(\omega, v \cdot P, P^2) + \\ - \frac{1}{4} J_0(\omega - v \cdot P) + \left(\frac{P^2 - 2\omega(v \cdot P)}{8\vec{P}^2} \right) (J_0(\omega) - J_0(\omega - v \cdot P)) + \\ + \frac{v \cdot P - 2\omega}{2(4\pi)^2} + \mathcal{O}(4-d). \quad (16)$$

$$M_{\text{IV}} = \frac{g_A^3}{4f_\pi^5} \sum_{i \neq j=1,2} \frac{S_j \cdot k_j}{k_j^2 - m_\pi^2 + i\eta} \\ \times \{ (-m_\pi^2 + (v \cdot p_i)^2) J_0(v \cdot p_i) + (-m_\pi^2 + (v \cdot p'_i)^2) J_0(v \cdot p'_i) + \\ + v \cdot (p_i + p'_i) \Delta_\pi + [3k_i^2 - m_\pi^2 - 2k_i \cdot q] X \}, \quad (17)$$

where

$$X = -\frac{v \cdot (p_i + p'_i)}{2} I_\pi(k_i) + \left(m_\pi^2 - v \cdot p_i v \cdot p'_i - \frac{1}{2} k_i^2 \right) I_0(v \cdot p_i, v \cdot k_i, k_i^2) - \frac{1}{2} [J_0(v \cdot p_i) + J_0(v \cdot p'_i)]. \quad (18)$$

$$M_V = \frac{g_A^3}{4f_\pi^5} \sum_{i \neq j=1,2} \frac{-S_j \cdot k_j}{k_j^2 - m_\pi^2 + i\eta} \times \{ v \cdot (p_i + p'_i) \Delta_\pi + ((v \cdot p_i)^2 - m_\pi^2) J_0(v \cdot p_i) + ((v \cdot p'_i)^2 - m_\pi^2) J_0(v \cdot p'_i) \}. \quad (19)$$

$$M_{VI} = \frac{g_A}{8f_\pi^5} \sum_{i \neq j=1,2} \frac{-S_j \cdot k_j}{k_j^2 - m_\pi^2 + i\eta} \times \{ v \cdot (p_i + p'_i) \Delta_\pi + v \cdot (2q + p'_i) v \cdot (-k_i + 2q + p'_i) J_0(v \cdot (p'_i + q)) + v \cdot (2q - p_i) v \cdot (-k_i + 2q - p_i) J_0(v \cdot (p_i - q)) \}. \quad (20)$$

As mentioned earlier, the graph in Fig.5 with the relevant lowest order vertices gives $\mathcal{T}^{(+1)}$ [eq.(5)]. If we, however, use for the pion rescattering vertex in Fig.5 the lagrangian $\mathcal{L}^{(2)}$ [21], there results an NNLO transition operator, M_{VII} , which represents “recoil” term corrections of $\mathcal{O}(m_N^{-2})$ to $\mathcal{T}^{(+1)}$. Its explicit expression is

$$M_{VII} = \left(-\frac{g_A}{f_\pi} \right) \sum_{i \neq j=1,2} \kappa'_i(k_j, q) \frac{\vec{\sigma}_j \cdot \vec{k}_j \tau_j^0}{k_j^2 - m_\pi^2 + i\eta} \quad (21)$$

where the expression for $\kappa'_i(k_j, q)$ is obtainable from Eq.(C.3) of Ref. [21].

The above expressions for the $\nu = 2$ diagrams contain four independent one-loop integrals, Δ_π , $J_0(\omega)$, $I_\pi(P^2)$ and $I_0(\omega, v \cdot P, P^2)$, of which the first three contain divergences. The finite parts are defined to include $\ln(m_\pi/\lambda)$. We choose the cut-off parameter to be $\lambda = 1$ GeV. The two integrals, Δ_π and $J_0(\omega)$, can be found in Ref. [20], while $I_\pi(P^2)$ is a standard Feynman integral:

$$I_\pi(P^2) = \frac{1}{i} \int \frac{d^4 l}{(2\pi)^4} \frac{1}{[m^2 - l^2 - i\varepsilon][m^2 - (l - P)^2 - i\varepsilon]}. \quad (22)$$

The last integral, which is new, is given by

$$\begin{aligned} I_0(\omega, v \cdot P, P^2) &= \frac{1}{i} \int \frac{d^4 l}{(2\pi)^4} \frac{1}{(v \cdot l - \omega - i\varepsilon)(m_\pi^2 - l^2 - i\varepsilon)[m_\pi^2 - (l - P)^2 - i\varepsilon]} \\ &= \frac{1}{16\pi^2} \int_0^1 dx \left[\theta(s) \frac{2}{\sqrt{s}} \left(\frac{\pi}{2} + \tan^{-1} \frac{\xi}{\sqrt{s}} \right) + \theta(-s) \frac{1}{\sqrt{-s}} \log \left| \frac{\xi - \sqrt{-s}}{\xi + \sqrt{-s}} \right| \right] + \\ &\quad + i \frac{1}{16\pi} \int_0^1 dx \frac{\theta(-s)}{\sqrt{-s}} [\theta(\xi + \sqrt{-s}) + \theta(\xi - \sqrt{-s})], \end{aligned} \quad (23)$$

where $s = m^2 - \omega^2 + x(2\omega P_0 - P^2) + x^2(P^2 - P_0^2)$, $P_0 = v \cdot P$ and $\xi = \omega - x P_0$. $I_0(\omega, v \cdot P, P^2)$ reduces to the integral $\gamma_0(v \cdot P)$ given in appendix B of Ref. [20] in the limit $\omega = 0$ and $P^2 = 0$. This limit, however, is not applicable to the $pp \rightarrow pp\pi^0$ reaction.

Our NNLO diagrams contain the usual divergences which need to be regularized and then renormalized by appropriate counter terms. The single-nucleon process (Born term) of Fig.1(a) receives two types of corrections: (i) the finite “recoil corrections” of $\mathcal{O}(m_N^{-2})$ involving finite known parameters, and (ii) the (infinite) loop corrections. The $\nu = 1$ loop corrections, $\mathcal{T}_{corr}^{(+1)}$, to the Born amplitude were discussed in Ref. [13]. We denote by $\mathcal{T}_{corr}^{(+2)}$ the $\nu = 2$ loop and recoil corrections to the Born term. The recoil corrections to the Born term are reduced by $(m_\pi/m_N)^{\nu+2}$. The divergences contained in the graphs in Fig. 2 are canceled (“renormalized”) by counter-terms in $\mathcal{L}^{(2)}$ corresponding to the five-point ($\pi N N N N$) vertex diagram (Fig.6). The same terms renormalize a part of the singularities in M_{IV} , Eq.(17), coming from Fig.3. The remaining singularities in M_{IV} are similar to those in the graphs in Fig.4. To eliminate the latter singularities, $\mathcal{L}^{(2)}$ must contain further counter-terms of the pion-nucleon scattering vertex type [21]. This can be accomplished with the use of these counter-terms in graphs similar to the one in Fig.5. We let $\mathcal{T}_{corr}'^{(+2)}$ stand for the $\nu = 2$ transition operators that originate from such $\nu = 2$ counter-terms. The complete set of the $\nu = 2$ transition operators includes $\mathcal{T}_{corr}^{(+1)}$, $\mathcal{T}_{corr}^{(+2)}$, and $\mathcal{T}_{corr}'^{(+2)}$, but we defer detailed discussion of these terms to a forthcoming paper [19] and concentrate here on the finite parts of the following effective operators ¹

$$\mathcal{T} = \mathcal{T}^{Resc} + \mathcal{T}^{(+2)}. \quad (24)$$

d. Numerical results and discussion The purpose of this section is purely illustrative: we wish to have some idea as to the size of these corrections. A proper treatment of the derived transition operators must involve DW analyses, which we postpone to the forthcoming paper [19], where DW modifications to our numerical estimates described below as well as changes due to the use of a non-static nucleon propagator will be discussed.

To proceed, we must fix the free parameters of the previous expressions. To NLO, as discussed in Ref. [13,14], the three parameters, c_1 , c_2 and c_3 of Eq.(6), enter into the pion rescattering operator \mathcal{T}^{Resc} . We shall use the three sets of parameters employed in Ref. [15]. Sets A, B and C in Table 1 summarize these values. Set A represents the central values of c_1 , c_2 and c_3 determined in Ref. [20] using the experimental values of the pion-nucleon σ term, the nucleon axial polarizability α_A and the isospin-even s-wave πN scattering length a^+ . Sets B and C represent typical ranges of allowed values in the current determinations of these parameters (see Ref. [13] for details).

For simplicity we limit our consideration to the *threshold kinematics*, which means $q^\mu = (m_\pi, \vec{0})$ and the single exchanged boson (pion) of Fig. 1(b) has the four-momentum $k^\mu = (m_\pi/2, \vec{k})$ with $k^2 = -m_\pi m_N$. Then the final nucleon three momenta are $\vec{p}_i' = 0$ (for nucleon $i = 1, 2$), and $\kappa(k, q)$ in Eq.(6) is fixed at [13,14]

$$\kappa_{th} = \frac{m_\pi^2}{f_\pi^2} \left(2c_1 - \frac{1}{2}(c_2 + c_3 - \frac{g_A^2}{8m_N}) \right). \quad (25)$$

Quantities of interest here are the magnitudes of the finite parts of the $\nu = 2$ transition operators, Eqs.(8)-(20), relative to the magnitude of the pion rescattering operator, \mathcal{T}^{Resc} ,

¹Since we do not consider DW we leave out \mathcal{T}^{Born}

Eq. (5). Let us denote these ratios ² by $R_K \equiv M_K/\mathcal{T}^{Resc}$ ($K = \text{I, II, III, } \dots, \text{VII}$). Table 2 gives R_K 's for each of the parameter sets A, B, and C. We note that R_I , R_{II} and R_{III} , corresponding to the graphs in Fig. 2, give quite substantial individual contributions but R_{II} and R_{III} cancel each other at threshold.³ Most remarkably, R_{IV} corresponding to the pion-pion rescattering diagram, Fig.3, is large, ranging $5 \sim 10$.

The appearance of these large individual contributions calls for an explanation. The two-pion exchange diagrams in Figs. 2 and 3 all involve one-loop integrals with three or four propagators. These loop integrals, for which typical four-momentum transfers k are large, can produce the factor $k^2 = -m_\pi m_N$ in the numerator multiplying the integral $I_0(\omega, v \cdot P, P^2)$ of eq.(23). This factor turns out to be accompanied by some negative powers of f_π^2 coming from the vertices, resulting in a large enhancement factor, $\mathcal{O}(k^2 f_\pi^{-2} = -m_\pi m_N f_\pi^{-2} \simeq -15)$. This feature essentially explains the large size of the two-pion exchange diagrams, although there are other diagram-specific numerical factors.

The two-pion exchange diagrams in Fig. 2 can perhaps be viewed as a part of an effective σ -meson exchange that Lee and Riska [4] found to be important in $pp \rightarrow pp\pi^0$. It has been shown via soft-pion arguments [23] that the effective σ -meson exchange can be understood as a two-pion exchange. The results in Ref. [23] lead us to suspect that the few diagrams we consider here are insufficient to generate the full strength of isoscalar two-pion exchange between two nucleons, but our NNLO results are indicative of the importance of the two-pion exchange diagrams for $pp \rightarrow pp\pi^0$. Similar HB χ PT two-pion exchange diagrams have been considered in calculating the scattering amplitudes for higher partial waves in NN collision [24]. It is to be noted, however, that the higher partial wave amplitudes, which are only sensitive to peripheral NN scattering, can probe two-pion exchange contributions only for low three-momentum transfers. By contrast, in the $NN \rightarrow NN\pi$ reaction, the two-pion exchange diagrams are probed in a very different kinematical regime of “high” energy- and three-momentum transfers between the two nucleons. It is therefore not surprising that the roles of the two-pion exchange diagrams in our calculation are very different from those discussed in Ref. [24].

The diagrams shown in Fig. 4 generate effective form factors at the pion-nucleon rescattering vertex in $\mathcal{T}^{(+1)}$. According to Table 2, the contributions of the corresponding operators, R_V and R_{VI} , are less than 20% and 15% , respectively. Thus, the higher chiral-order vertex corrections to $\mathcal{T}^{(+1)}$ are found to be small, as expected from the general tenets of χ PT. Meanwhile, Table 2 shows that $R_{VII} = -1.7 \sim -2.3$. This means that the combined pion recattering term, given by the sum of Fig.1(b) and the Type VII contribution, has the same sign as the Born term, Fig.1(a). This indicates that the sign problem encountered in the previous χ PT calculations [13,15] might be resolved by higher order effects.

Gedalin *et al.* [22] considered some NNLO diagrams within HB χ PT. Numerically, they have found that the sum of M_{IV} and M_V (in our notation) is large. This feature is confirmed

² This type of comparison is possible because, at threshold, effectively only one kind of spin operator appears in the $pp \rightarrow pp\pi^0$ transition operator.

³ With DW this cancellation will not occur due to the different energy and three-momentum dependences.

by our numerical result. It is worth emphasizing, however, that of these two operators M_{IV} is by far the predominant one. Although Gedalin *et al.* also considered M_{II} (our notation), they left out M_I and M_{III} . According to Table 2, M_{II} and M_{III} are of equal importance, and their individual contributions are comparable to that of M_{IV} . Our final remark is that our results contain a new loop-integral $I_0(\omega, v \cdot p, p^2)$, Eq. (23), which does not appear in Ref. [22].

e. Conclusions We have evaluated the $pp \rightarrow pp\pi^0$ transition operators to NNLO in chiral expansion. It was found that χ PT vertex corrections to the lower chiral order transition operators, \mathcal{T}^{Born} and \mathcal{T}^{Resc} are indeed small. Thus, for this limited type of diagrams, χ PT expansion seems to be under control. Meanwhile, the two-pion exchange contributions are found to be very large in our estimates. This result is consistent with the expectation that the $pp \rightarrow pp\pi^0$ reaction is sensitive to “heavy”-meson exchanges between nucleons. The phenomenologically important σ -meson contributions [4] seem to have discernible “representatives” among the NNLO chiral perturbation diagrams considered here. It is not obvious whether one can interpret the large contributions from the individual graphs in Figs. 2 and 3 as evidence for the non-convergence of the χ PT expansion. These types of graphs make their *first appearance* only in the NNLO calculations, and therefore the convergence question can only be settled by calculating corrections to these NNLO diagrams. We expect that the loop corrections to the individual diagrams in Fig.2 will be smaller in magnitude. However, two-pion exchange diagrams of chiral order $\nu = 3$ might have magnitudes comparable to our $\nu = 2$ terms since the diagrams in Fig.2 are only part of the effective σ - exchange.

To simulate more realistic σ -exchange it may also be necessary to explicitly include intermediate Δ -particles in Figs. 2 and 3, but that would require a thorough recalculation of many previous results. In a forthcoming paper [19] we hope to present a detailed discussion of DW calculations which are required to obtain realistic cross sections for $pp \rightarrow pp\pi^0$, as well as the details of a renormalization procedure relevant to an NNLO calculation. Due to large energy-momentum transfers involved in the $NN \rightarrow NN\pi$ reaction, a full DW calculation can modify significantly the numerical results reported in this Letter. Our finding that the “recoil” corrections $\mathcal{O}(m_N^{-1})$ to \mathcal{T}^{Resc} are large points to the necessity of examining the use of the static heavy-baryon “propagator”, $1/(v \cdot p)$. As a first pragmatic step, one can think of replacing $1/(v \cdot p)$ with $1/(v \cdot p - \vec{p}^2/(2m_N))$, which implies, however, an extension of HB χ PT adopted in this work.

We thank Shung-ichi Ando for pointing out an error in our calculation of the recoil correction to the pion rescattering diagram. This work is supported in part by the National Science Foundation, Grant No. PHYS-9602000 and by the Grant-in-Aid of Scientific Research, the Ministry of Education, Science and Culture, Japan, Contract No.07640405.

REFERENCES

- [1] H. O. Meyer *et al.*, Phys. Rev. Lett. **65**, 2846 (1990); Nucl. Phys. **A539**, 633 (1992).
- [2] A. Bondar *et al.*, Phys. Lett. B **356**, 8 (1995).
- [3] G. A. Miller and P. U. Sauer, Phys. Rev. C **44**, R1725 (1991); J.A. Niskanen, Phys. Lett. B **289**, 227 (1992).
- [4] T.-S. H. Lee and D. O. Riska, Phys. Rev. Lett. **70**, 2237 (1993).
- [5] C. J. Horowitz, H. O. Meyer and D. K. Griegel, Phys. Rev. C **49**, 1337 (1994).
- [6] E. Hernández and E. Oset, Phys. Lett. B **350**, 158 (1995).
- [7] C. Hanhart, J. Haidenbauer, A. Reuber, C. Schütz and J. Speth, Phys. Lett. B **358**, 21 (1995); Acta Phys. Pol. B **27**, 2893 (1996).
- [8] C. Hanhart, J. Haidenbauer, M. Hoffmann, U.-G. Meissner and J. Speth, Phys. Lett. B **424**, 8 (1998); C. Hanhart, J. Haidenbauer, O. Krehl and J. Speth, Phys. Lett. B **444**, 25 (1998).
- [9] R. Shyam and U. Mosel, Phys. Lett. B **426**, 1 (1998).
- [10] F. Kleefeld and M. Dillig, Acta Phys. Pol. B **29**, 3059 (1998).
- [11] V. Bernard, N. Kaiser and U.-G. Meissner, Eur. J. Phys. A **4**, 259 (1999); see also E. Gedalin, A. Moalem and L. Razdolskaya, preprint nucl-th/9812009 (1998).
- [12] J. Adam, A. Stadler, M.T. Pena and F. Gross, Phys. Lett. B **407**, 97 (1997).
- [13] B.-Y. Park, F. Myhrer, T. Meissner, J.R. Morones, K. Kubodera, Phys. Rev. C **53**, 1519 (1996).
- [14] T.D. Cohen, J.L. Friar, G.A. Miller and U. van Kolck, Phys. Rev. C **53**, 2661 (1996).
- [15] T. Sato, T.-S. Lee, F. Myhrer and K. Kubodera, Phys. Rev. C **56**, 1246 (1997).
- [16] U. van Kolck, G. A. Miller and D. O. Riska, Phys. Lett. B **388**, 679 (1996).
- [17] E. Jenkins and A. V. Manohar, Phys. Lett. B **255**, 558 (1991).
- [18] S. Weinberg, Phys. Lett. B **251**, 288 (1990); Nucl. Phys. **B363**, 3 (1991); Phys. Lett. **B295**, 114 (1992).
- [19] V. Dmitrašinović K. Kubodera, F. Myhrer and T. Sato, in preparation.
- [20] V. Bernard, N. Kaiser and Ulf-G. Meissner, Int. J. Mod. Phys. **E4**, 193 (1995).
- [21] N. Fettes, U.-G. Meissner and S. Steininger, Nucl. Phys. **A640**, 199 (1998).
- [22] E. Gedalin, A. Moalem and L. Razdolskaya, preprint nucl-th/9803029 (1998).
- [23] See e.g., G.E. Brown and J. Durso, Phys. Lett. B **35**, 120 (1971); G.E. Brown, in “Mesons in Nuclei”, eds. M.Rho and D. Wilkinson (North-Holland, Amsterdam, 1979), 329.
- [24] N. Kaiser, R. Brockmann and W. Weise, Nucl. Phys. **A625**, 758 (1997); N. Kaiser, S. Gerstendörfer and W. Weise, Nucl. Phys. **A637**, 395 (1998); M.C.M Rentmeester et al., nucl-th/9901054

TABLES

TABLE I. The three sets of $c_{1,2,3}$ parameters, in units of GeV^{-1} , used in the text.

	c_1	c_2	c_3
A	-0.87	3.34	-5.25
B	-0.87	4.5	-5.25
C	-0.98	3.34	-5.25

TABLE II. Sizes of the K^{th} type of diagrams, shown in Figs. 2 - 5, relative to the $\nu = 1$ pion rescattering diagram, Fig. 1(b). The ratio R_K defined in the text is given for three sets (A, B and C) of parameters ($c_{1,2,3}$), see the text and Table 1.

	R_K^{A}	R_K^{B}	R_K^{C}
$K = \text{I}$	-0.70	-0.38	-0.53
$K = \text{II}$	6.7	3.6	5.1
$K = \text{III}$	-6.7	-3.6	-5.1
$K = \text{IV}$	9.5	5.1	7.2
$K = \text{V}$	0.18	0.10	0.14
$K = \text{VI}$	0.14	0.08	0.11
$K = \text{VII}$	-2.3	-1.7	-1.7

FIGURES

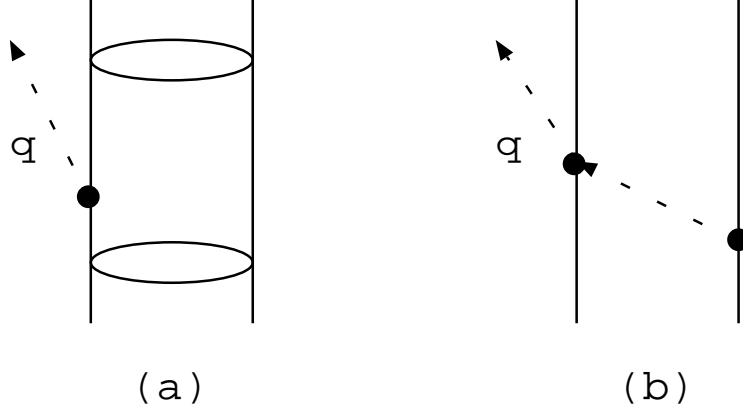
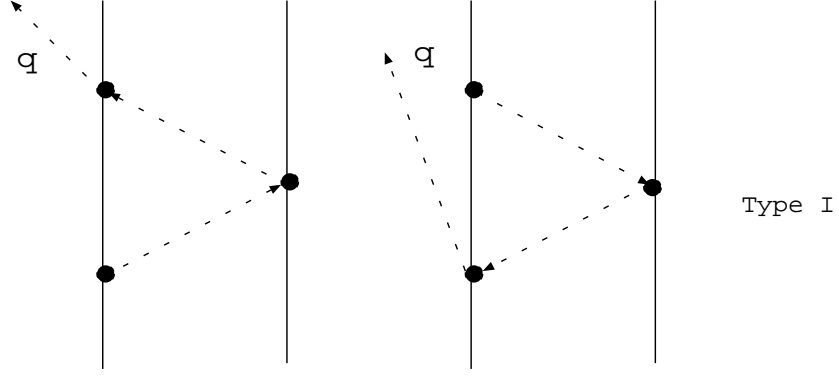
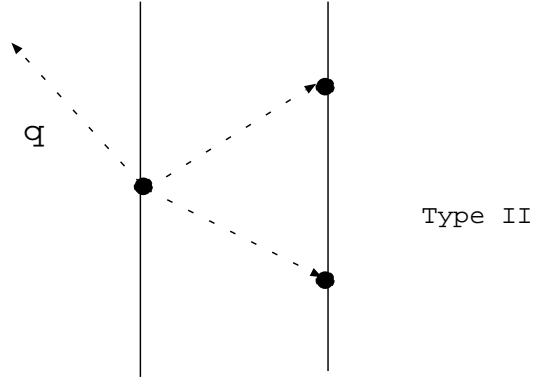


FIG. 1. Diagrams contributing to $pp \rightarrow pp\pi^0$: Born term (a), the pion-rescattering term (b). The solid line denotes a nucleon (proton), the dashed line a pion and the open ellipses denote initial-/final-state interactions.



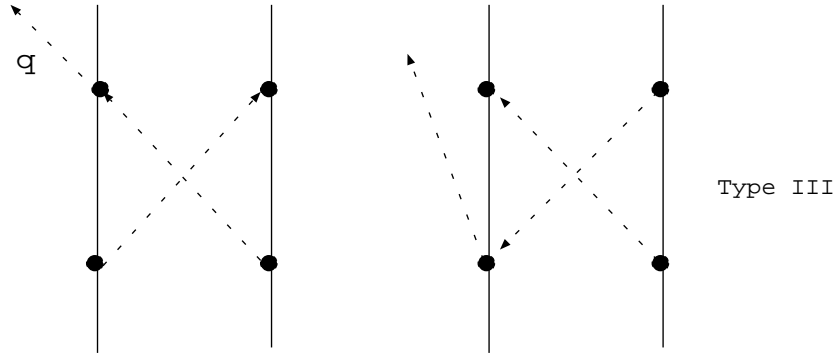
Type I

(a)



Type II

(b)



Type III

(c)

FIG. 2. Two-pion exchange graphs of type I, II and III -the “cross-box” graphs.

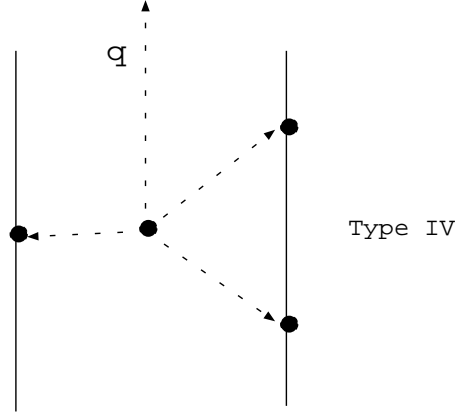


FIG. 3. Pion-pion s-wave rescattering graph of type IV.

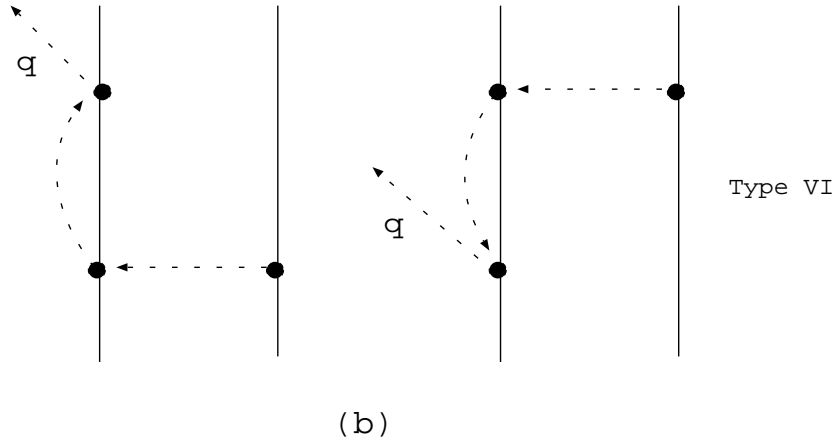
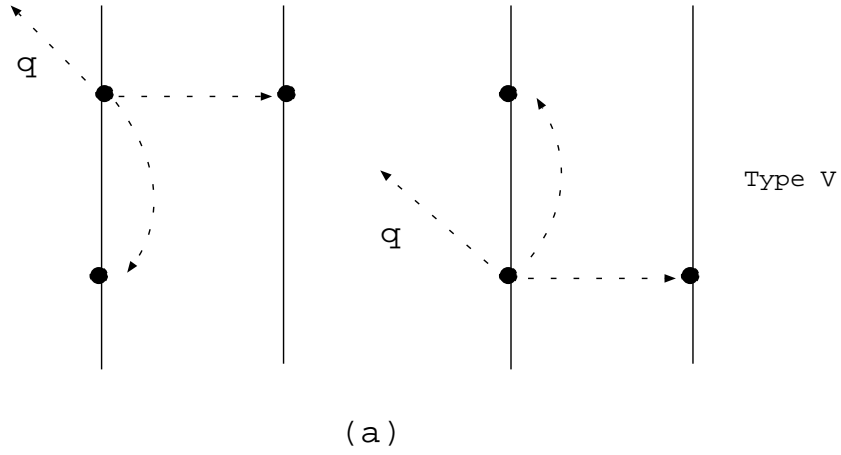


FIG. 4. Pion rescattering vertex corrections to Fig.1(b) of type V and VI.

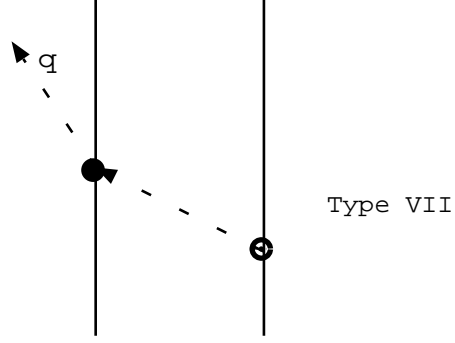


FIG. 5. The pion-rescattering graph with $\bar{\nu} = 2$ at rescattering vertex.

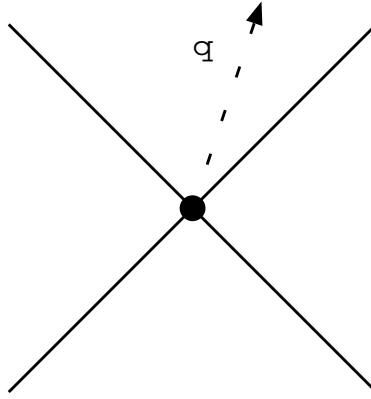


FIG. 6. The five-point contact-interaction counter-term graph.